

Supporting Information for

Underlying Mechanisms on Synergistic Role of Li_2MnO_3 and $\text{LiNi}_{1/3}\text{Co}_{1/3}\text{Mn}_{1/3}\text{O}_2$ in High-Mn, Li- rich Oxides

Jin-Myoung Lim,^a Duho Kim,^a Min-Sik Park,^{b,d} Maenghyo Cho,^{,a} and Kyeongjae Cho^{*,a,c}*

^a Department of Mechanical and Aerospace Engineering, Seoul National University, Gwanak-ro 1, Gwanak-gu, Seoul 08826, Republic of Korea.

^b Advanced Batteries Research Center, Korea Electronics Technology Institute, 25 Saenari-ro, Bundang-gu, Seongnam, 13509, Republic of Korea.

^c Department of Materials Science and Engineering and Department of Physics, the University of Texas at Dallas, Richardson, TX 75080, USA.

^d Department of Advanced Materials Engineering for Information and Electronics, Kyung Hee University, 1732 Deogyong-daero, Giheung-gu, Yongin 17104, Republic of Korea.

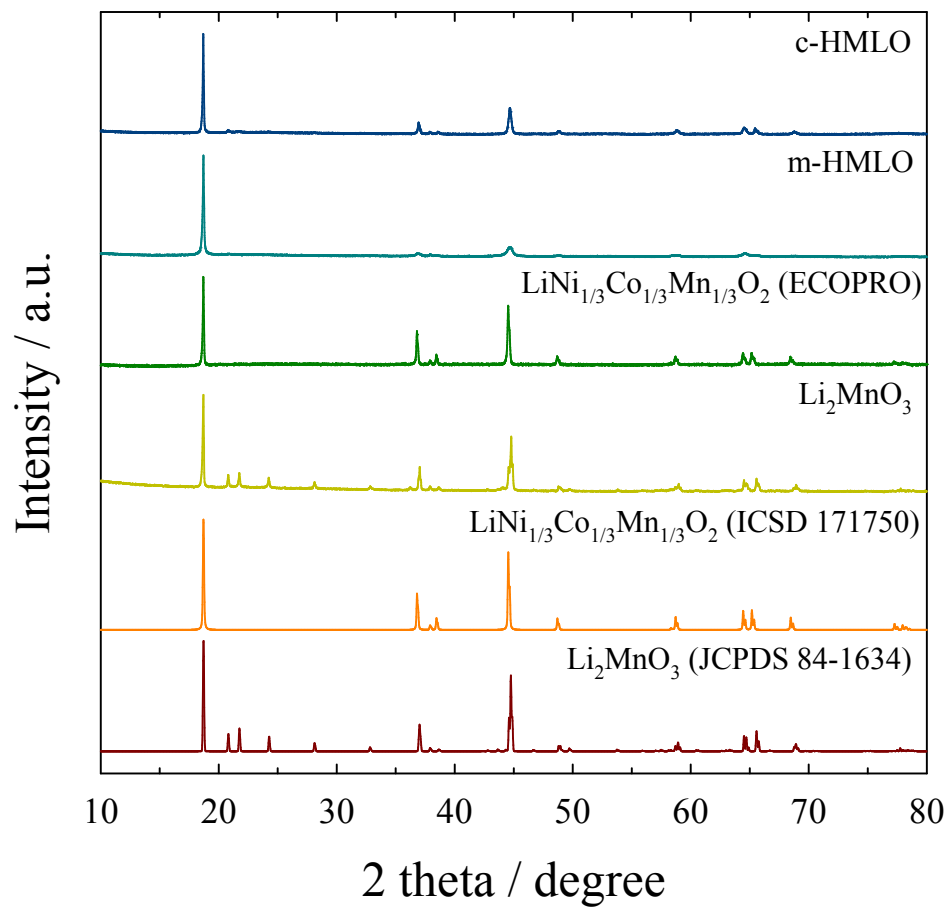


Figure S1. Powder XRD patterns of reference Li₂MnO₃ (JCPDS 84-1634), reference LiNi_{1/3}Co_{1/3}Mn_{1/3}O₂ (ICSD 171750), as-synthesized Li₂MnO₃, commercialized LiNi_{1/3}Co_{1/3}Mn_{1/3}O₂ (ECOPRO), m-HMLO, and c-HMLO.

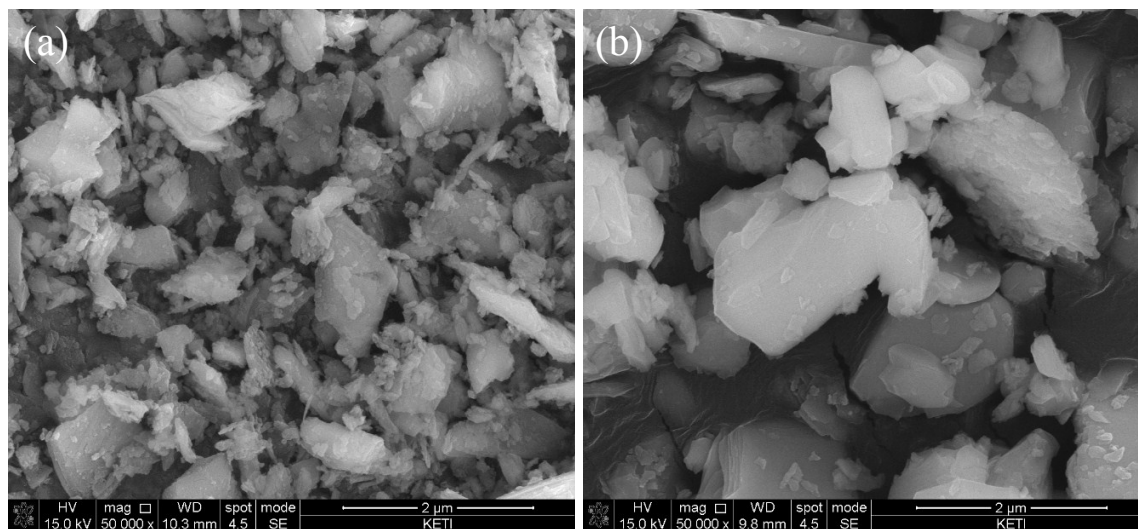


Figure S2. FESEM images of m-HMLO (a) and c-HMLO (b).

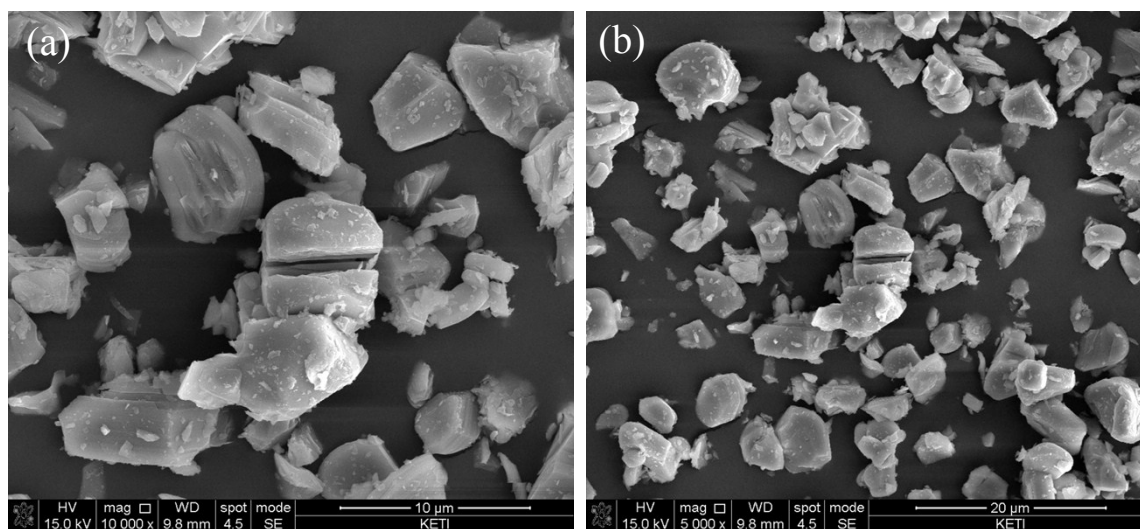


Figure S3. Field-emission scanning electron microscope (FESEM) images of as-synthesized Li_2MnO_3 at low magnification (a) and high magnification (b).

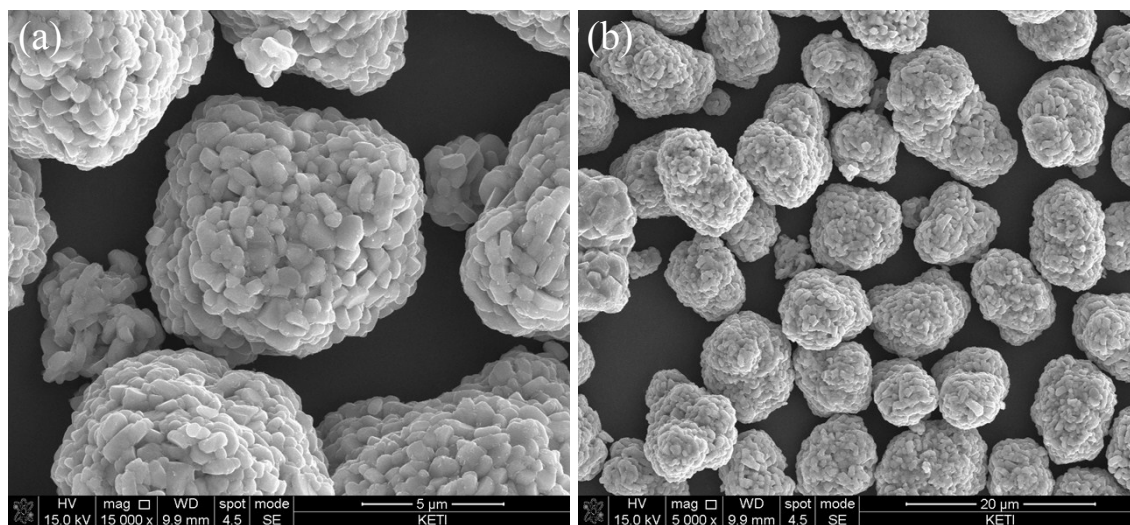


Figure S4. Field-emission scanning electron microscope (FESEM) images of commercialized $\text{LiNi}_{1/3}\text{Co}_{1/3}\text{Mn}_{1/3}\text{O}_2$ at low magnification (a) and high magnification (b).

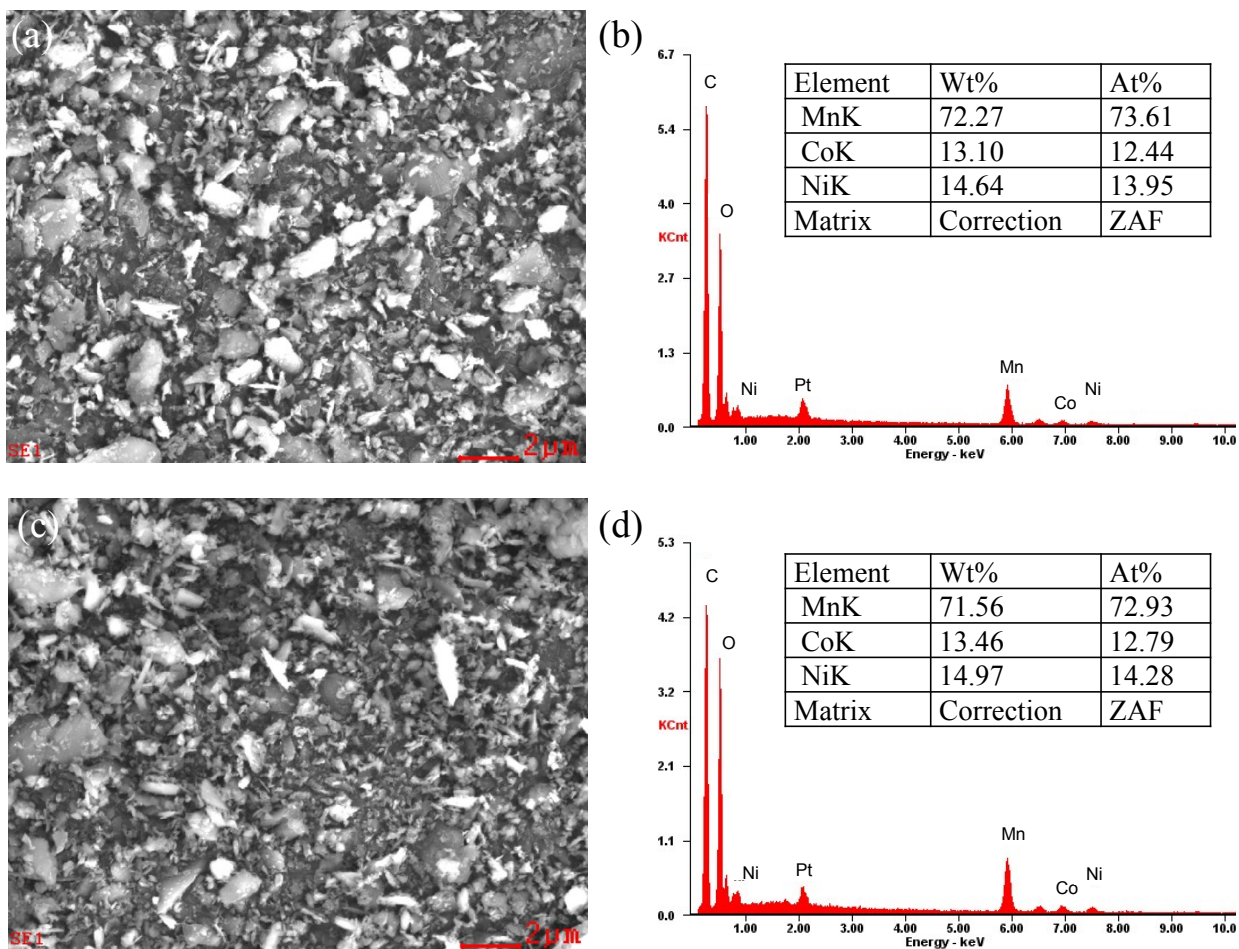


Figure S5. (a, c) FESEM images of m-HMLO at different two locations; (b, d) EDS patterns with the corresponding composition table.

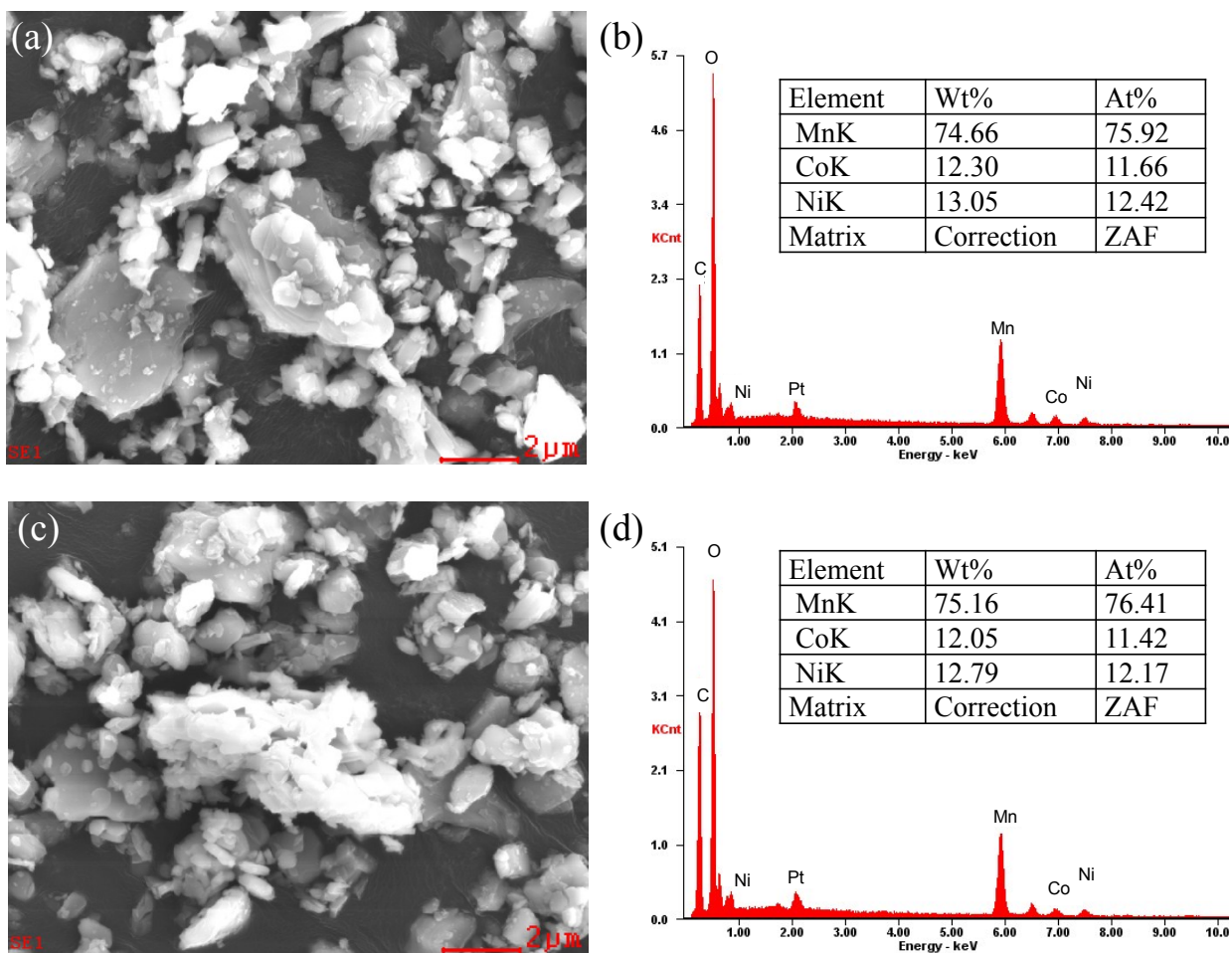


Figure S6. (a, c) FESEM images of c-HMLO at different two locations; (b, d) EDS patterns with the corresponding composition table.

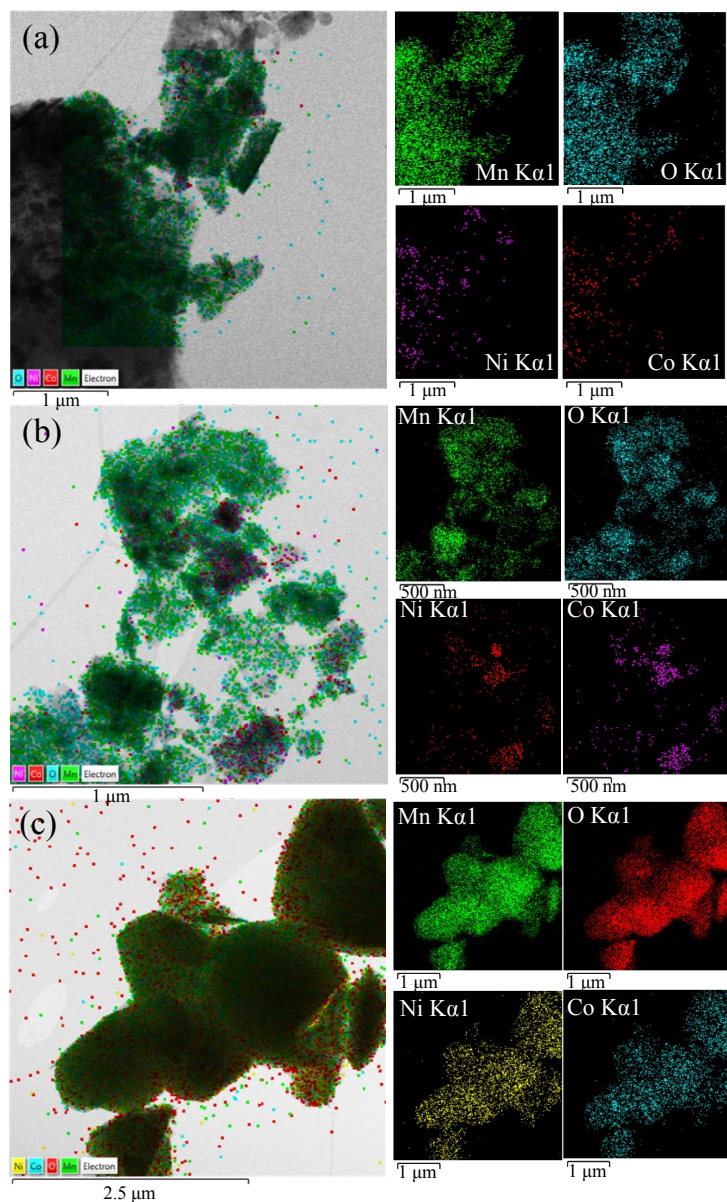


Figure S7. (a, b) STEM images of as-prepared m-HMLO with EDS elemental mapping of Mn (green), O (cyan), Ni (purple), and Co (red) in two different regions. (c) STEM image of as-prepared c-HMLO with EDS elemental mapping of Mn (green), O (red), Ni (yellow), and Co (cyan).

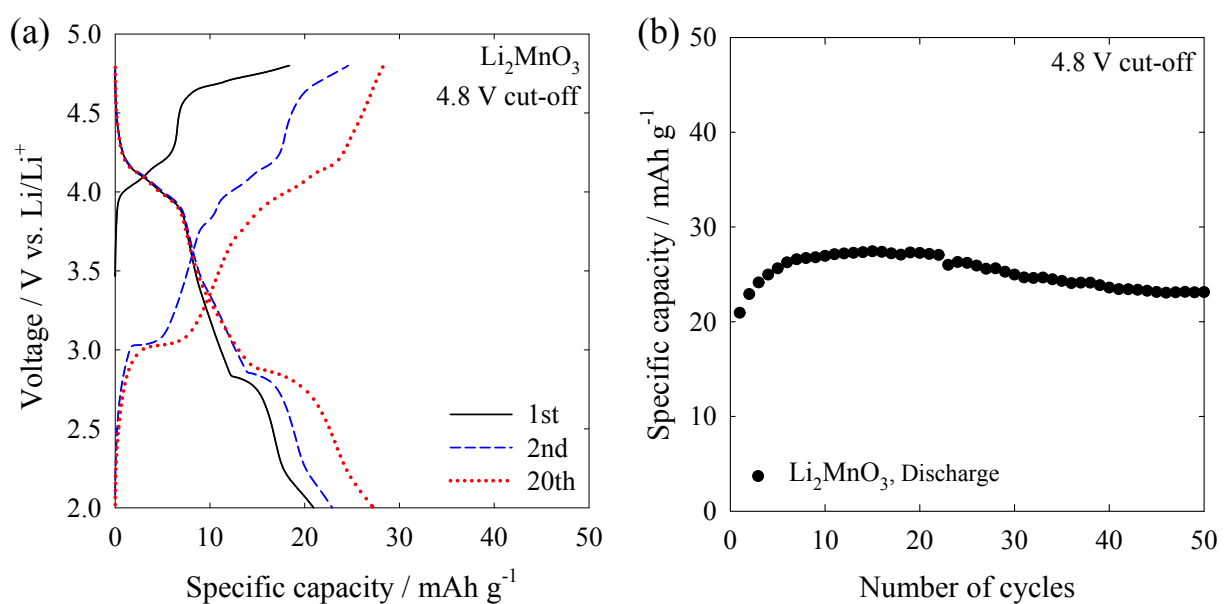


Figure S8. (a) Galvanostatic charge-discharge profiles of as-synthesized Li₂MnO₃, recorded in constant-current (CC) charging mode at a constant specific current of 13 mA g⁻¹, in the voltage range between 2.0 and 4.8 V vs. Li/Li⁺ at 1st, 2nd, and 20th cycles. (b) Discharge (filled black circles) cyclic performance of as-synthesized Li₂MnO₃.

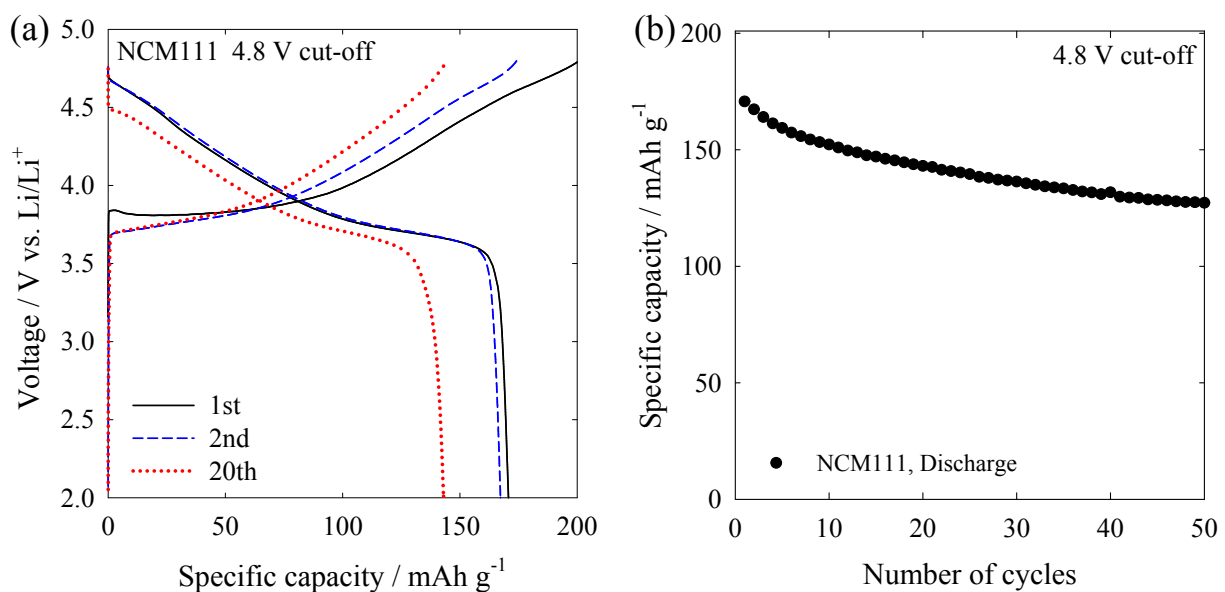


Figure S9. (a) Galvanostatic charge-discharge profiles of commercialized $\text{LiNi}_{1/3}\text{Co}_{1/3}\text{Mn}_{1/3}\text{O}_2$ (NCM111) recorded in constant-current (CC) charging mode at a constant specific current of 25 mA g^{-1} , in the voltage range between 2.0 and 4.8 V vs. Li/Li^+ at 1st, 2nd, and 20th cycles. (b) Discharge (filled black circles) cyclic performance of commercialized $\text{LiNi}_{1/3}\text{Co}_{1/3}\text{Mn}_{1/3}\text{O}_2$.

Table S1. Comparison of structural parameters of as-prepared c-HMLO obtained from Rietveld refinement and the atomic model of $\text{Li}_{1.67}\text{Ni}_{0.11}\text{Co}_{0.11}\text{Mn}_{0.67}\text{Cu}_{0.11}\text{O}_{2.67}$, obtained by density functional theory (DFT) calculation.

	a [Å]	b [Å]	c [Å]	β [°]
Rietveld	4.9369	17.0907	5.0268	109.29
DFT	5.0076	17.3247	5.0867	109.42

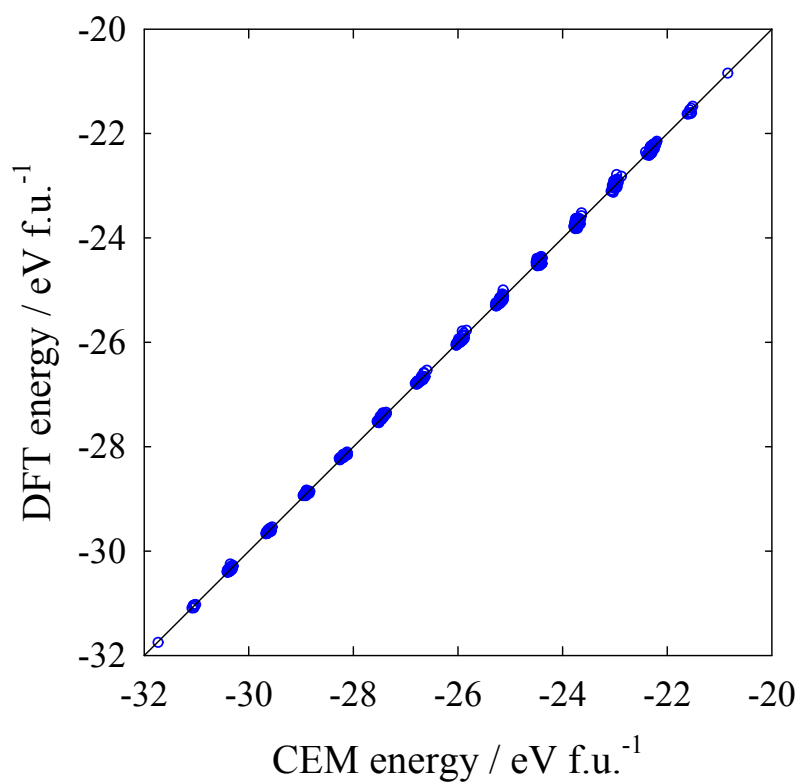


Figure S10. Total energy predicted by the cluster expansion method (CEM) vs. total energy calculated by density functional theory (DFT) for the same configuration (average root mean square error: 0.102 %).

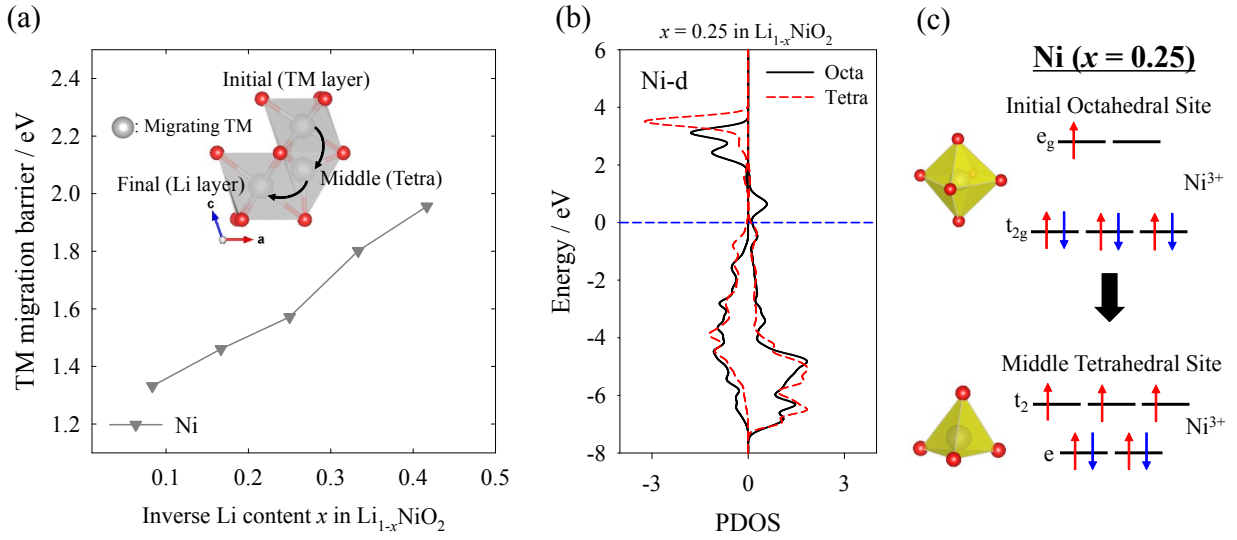


Figure S11. (a) Migration barriers of Ni ions with respect to the inverse Li content x in $\text{Li}_{1-x}\text{NiO}_2$ from the initial TM layer to the final Li layer *via* the middle tetrahedral site (inset). (b) PDOS for Ni d-orbital at the initial octahedral site (black solid line) and middle tetrahedral site (red dashed line) at $\text{Li}_{0.75}\text{NiO}_2$, where the Fermi level is 0.0 eV (blue dashed line). (c) Corresponding CFSDs of Ni d-orbitals at the initial octahedral site (upper) and middle tetrahedral site (lower) for $\text{Li}_{0.75}\text{NiO}_2$.